ORIGINAL ARTICLE

OPEN

Overexpression of HMGB1 in hepatocytes accelerates PTEN inactivation-induced liver cancer

Dipti Athavale[1] | Inés Barahona[1] | Zhuolun Song[1] | Romain Desert[1] | Wei Chen[1] | Hui Han[1] | Sukanta Das[1] | Xiaodong Ge[1] | Sai Santosh B. Komakula[1] | Shenglan Gao[1] | Daniel Lantvit[1] | Grace Guzman[1] | Natalia Nieto[1,2]

[1]Department of Pathology, University of Illinois at Chicago, Chicago, Illinois, USA

[2]Department of Medicine, Division of Gastroenterology and Hepatology, University of Illinois at Chicago, Chicago, Illinois, USA

Correspondence
Natalia Nieto, Department of Pathology, University of Illinois at Chicago, 840 S, Wood St., Suite 130 CSN, MC 847, Chicago, IL 60612, USA.
Email: nnieto@uic.edu

Abstract

Background: Liver cancer is increasing due to the rise in metabolic dysfunction-associated steatohepatitis (MASH). High-mobility group box-1 (HMGB1) is involved in the pathogenesis of chronic liver disease, but its role in MASH-associated liver cancer is unknown. We hypothesized that an increase in hepatocyte-derived HMGB1 in a mouse model of inactivation of PTEN that causes MASH could promote MASH-induced tumorigenesis.

Methods: We analyzed publicly available transcriptomics datasets, and to explore the effect of overexpressing HMGB1 in cancer progression, we injected 1.5-month-old $Pten^{\triangle Hep}$ mice with adeno-associated virus serotype-8 (AAV8) vectors to overexpress HMGB1-EGFP or EGFP, and sacrificed them at 3, 9 and 11 months of age.

Results: We found that HMGB1 mRNA increases in human MASH and MASH-induced hepatocellular carcinoma (MASH-HCC) compared to healthy livers. Male and female $Pten^{\triangle Hep}$ mice overexpressing HMGB1 showed accelerated liver tumor development at 9 and 11 months, respectively, with increased tumor size and volume, compared to control $Pten^{\triangle Hep}$ mice. Moreover, $Pten^{\triangle Hep}$ mice overexpressing HMGB1, had increased incidence of mixed HCC-intrahepatic cholangiocarcinoma (iCCA). All iCCAs were positive for nuclear YAP and SOX9. Male $Pten^{\triangle Hep}$ mice overexpressing HMGB1 showed increased cell proliferation and F4/80+ cells at 3 and 9 months.

- -

Conclusion: Overexpression of HMGB1 in hepatocytes accelerates liver tumorigenesis in $Pten^{\triangle Hep}$ mice, enhancing cell proliferation and F4/80+ cells to drive MASH-induced liver cancer.

INTRODUCTION

Liver cancer is the third leading cause of cancer-related death, including HCC (~75% of cases), intrahepatic cholangiocarcinoma (iCCA) (~10% of cases), mixed HCC-iCCA, and other subtypes.[1,2] Metabolic dysfunction-associated steatotic liver disease is the fastest-growing cause of HCC.[3,4] Metabolic dysfunction-associated steatotic liver disease ranges from simple steatosis to metabolic dysfunction-associated steatohepatitis (MASH), the latter characterized by inflammation, fibrosis, and cirrhosis, increasing the risk of developing HCC[3,5] and iCCA.[6]

PTEN dephosphorylates phosphatidylinositol-3,4,5-triphosphate, produced by phosphoinositide-3-kinase (PI3K),[7,8] prevents downstream protein kinase B (AKT) phosphorylation (S473 and T308), and inhibits signaling pathways involved in cell cycle progression, metabolism, migration, and survival.[7] Mice with $Pten$ ablation in the liver ($Pten^{\triangle Hep}$) present a phenotype similar to human MASH and, by 11–16 months of age, develop HCC or mixed HCC-iCCA.[9] In human HCC, PTEN expression decreases or is absent, hyperactivating the PI3K-AKT signaling pathway.[7]

High-mobility group box-1 (HMGB1) is a nonhistone nuclear protein involved in chronic liver disease.[10] On hepatocyte injury, it undergoes nucleocytoplasmic shuttling, is secreted, and acts as a damage-associated molecular pattern.[10] Serum HMGB1 increases in patients with MASH,[11] and we showed that ablation of $Hmgb1$ in intestinal epithelial cells reduces MASH in mice.[12]

In this study, we hypothesized that an increase in hepatocyte-derived HMGB1 in a mouse model of inactivation of PTEN that causes MASH could promote MASH-induced tumorigenesis. We report that $Pten^{\triangle Hep}$ mice, overexpressing HMGB1 with an adeno-associated virus serotype-8 (AAV8) vector, show accelerated liver cancer. Although AKT activation, oxidative stress, and Wnt/β-catenin signaling remain unaffected, overexpression of HMGB1 increases cell proliferation and F4/80+ cells, both associated with accelerated tumorigenesis, compared to $Pten^{\triangle Hep}$ mice.

METHODS

General methodology

Details on general methodology, such as alanine aminotransferase activity, hematoxylin and eosin staining, immunohistochemistry, western blot analysis, mRNA isolation, and quantitative real-time PCR, are described.[13–19] Primer sequences are in Supplemental Table S1, http://links.lww.com/HC9/A645. Antibodies used for western blot analysis are in Supplemental Table S2, http://links.lww.com/HC9/A645. Reactions were developed using the Pierce ECL substrate (Thermo Fisher Scientific, Waltham, MA). Antibodies used for immunohistochemistry are in Supplemental Table S3, http://links.lww.com/HC9/A645. Reactions were developed using the Histostain Plus detection system (Thermo Fisher Scientific). The number of Ki67+ and F4/80+ cells in 10 fields at 200x was counted and averaged. Serum HMGB1 was measured by ELISA using a kit from Novus Biologicals (Littleton, CO). Reticulin staining was performed using a kit from Polysciences Inc. (Warrington, PA).

Mice

$Pten^{fl/fl}$ mice (JAX 004597) were purchased from the Jackson Laboratory (Bar Harbor, ME). The $Pten^{loxP}$ allele was created by inserting $loxP$ sites flanking exon 5 of $Pten$.[20] $Pten^{fl/fl}$ were bred with $Albumin\ (Alb).Cre$ (B6.Cg-Speer6-ps1$^{Tg(Alb-cre)21Mgn}$/J, JAX 003574) to generate $Pten^{\triangle Hep}$ mice. $Alb.Cre$ mice were used as controls.

AAV8 vectors

Male and female control and $Pten^{\triangle Hep}$ mice (1.5 months old) were injected with AAV8.Tbg.Hmgb1.EgGfp (Hmgb1 AAV8) to overexpress HMGB1 in hepatocytes or with AAV8.Tbg.Egfp (empty AAV8) as control.[21,22] Vectors were generated by the University of Pennsylvania Vector Core (Philadelphia, PA) and injected as a single dose (2.5e^{14} genome copies/mouse in 70 μL of sterile saline solution) through the retro-orbital vein.

Study approval

All animals received humane care according to the criteria outlined in the *Guide for the Care and Use of Laboratory Animals* prepared by the National Academy of Sciences and published by the National Institutes of Health. Housing and husbandry conditions were approved by the University of Illinois at Chicago Animal Care and Use Committee prior to the initiation of the studies. All *in vivo* experiments were carried out according to the *Animal Research: Reporting of In Vivo Experiments* guidelines.

Histological evaluation of liver tissues

Mice were sacrificed at the indicated times, body and liver weight measured, and liver-to-body weight ratios calculated. Tumor number, size, and total volume were logged. Livers were grossly examined, dissected at 0.5-cm intervals, processed, embedded, and sectioned at 0.4 μm thickness. Hematoxylin and eosin–stained paraffin-embedded sections were evaluated by a pathologist (Dr. Grace Guzman). Dysplastic hepatocytes were defined by presence of abnormal nuclear size, exhibiting small or large cell change, bizarre hyperchromatic or occasionally multiple nuclei, distribution in clusters, groups, or occupying an entire nodule, and absent liver cell plate expansion. Malignant hepatocytes, consistent with HCC, were identified by thickened liver cell plates, increased nucleocytoplasmic ratio, atypical vesicular nuclei, and when present, bile production. Tumors were evaluated for tumor type (HCC, iCCA, mixed HCC-iCCA) following the American Joint Committee on Cancer guidelines.[23] Tumor variants were defined as nonpleomorphic (usual variant), pleomorphic, and combined, according to the criteria outlined by Ferrell.[24,25] In addition, bile duct hamartomas and adenomas were noted.

Analysis of human data sets

HMGB1 expression was analyzed in microarray data set GSE164760 from patients with MASH-induced HCCs, adjacent nontumor MASH liver, MASH, healthy livers, and cirrhotic livers using probe "11739025_a_at" values. HMGB1 expression was further analyzed in RNA-sequencing (RNA-seq) data sets GSE126848 and GSE107943. Raw read counts from GSE126848 were normalized to fragments per Kilobase of transcript per million mapped reads values and further evaluated.

Statistics

Data are expressed as mean $\pm$ SEM. Statistical analysis between groups was performed by two-tailed Student t test. A $p < 0.05$ was considered significant.

RESULTS

HMGB1 expression increases in patients with MASH and liver cancer

Analysis of RNA-seq data set GSE126848 revealed that HMGB1 transcripts were increased in MASH compared to healthy livers (Figure 1A). Analysis of microarray data set GSE164760 unveiled increased HMGB1 mRNA in patients with MASH and MASH-induced HCC, compared to healthy livers, yet expression remained unchanged between MASH-tumor–adjacent and MASH-induced HCC (Figure 1B). We reported that HMGB1 expression is higher in primary liver cancer compared to healthy control in the human The Cancer Genome Atlas Liver Hepatocellular Carcinoma cohort.[26] Further analysis of RNA-seq data set GSE107943 from patients with iCCA showed increased expression of HMGB1 in tumor versus nontumor, irrespective of MASH (Figure 1C). Overall, these observations indicate that HMGB1 transcripts increase in patients with MASH and liver cancer.

Generation of $Pten^{\triangle Hep}$ mice overexpressing HMGB1

We next explored the effect of overexpressing HMGB1 in cancer progression using $Pten^{\triangle Hep}$ mice, known to develop MASH and liver cancer.[9,27] Pten deletion was confirmed by western blot and quantitative real-time PCR analysis (Supplemental Figure S1A, B, http://links.lww.com/HC9/A646). Overexpression of HMGB1 was achieved by retro-orbital injection of AAV8.Tbg.Hmgb1.Egfp (Hmgb1 AAV8) in control and $Pten^{\triangle Hep}$ mice. A separate cohort of mice was injected with AAV8.Tbg.Egfp (Empty AAV8) as control. Mice were followed for the development of tumors for 9 or 11 months (Figure 2A). Transduction efficiency was confirmed by PCR (Supplemental Figure S2A, B, http://links.lww.com/HC9/A647). Control and $Pten^{\triangle Hep}$ mice, transduced with Hmgb1 AAV8, showed hepatocytes with strong nuclear HMGB1 and EGFP staining at 9 and 11 months. Mice injected with empty AAV8 showed hepatocytes with diffused cytoplasmic EGFP staining and nuclei-positive for endogenous HMGB1, yet the staining intensity was weaker than in Hmgb1 AAV8-injected mice at 9 and 11 months (Figure 2B, Supplemental Figure S2C, D, http://links.lww.com/HC9/A647). Western blot analysis revealed slight induction of HMGB1 in liver lysates from Hmgb1 compared to empty AAV8-injected control and $Pten^{\triangle Hep}$ male mice at 9 months (Supplemental Figure S2E, http://links.lww.com/HC9/A647).

Overexpression of HMGB1 was also induced for 3 months (Supplemental Figure S3A, http://links.lww.com/HC9/A648). Liver-to-body weight ratio and steatosis remained similar in empty and Hmgb1 AAV8-injected male $Pten^{\triangle Hep}$ mice at 3 months (Supplemental Figure S3B, C, http://links.lww.com/HC9/A648). Empty AAV8-injected $Pten^{\triangle Hep}$ mice showed cytoplasmic EGFP staining, while Hmgb1 AAV8 injection led to nuclear EGFP staining (Supplemental Figure S3D, http://links.lww.com/HC9/A648). Furthermore, western blot analysis revealed a 1.8-fold induction of HMGB1 in Hmgb1 compared to empty AAV8-injected $Pten^{\triangle Hep}$ mice at 3 months (Figure 2C). Endogenous (host-derived) serum HMGB1 increased,
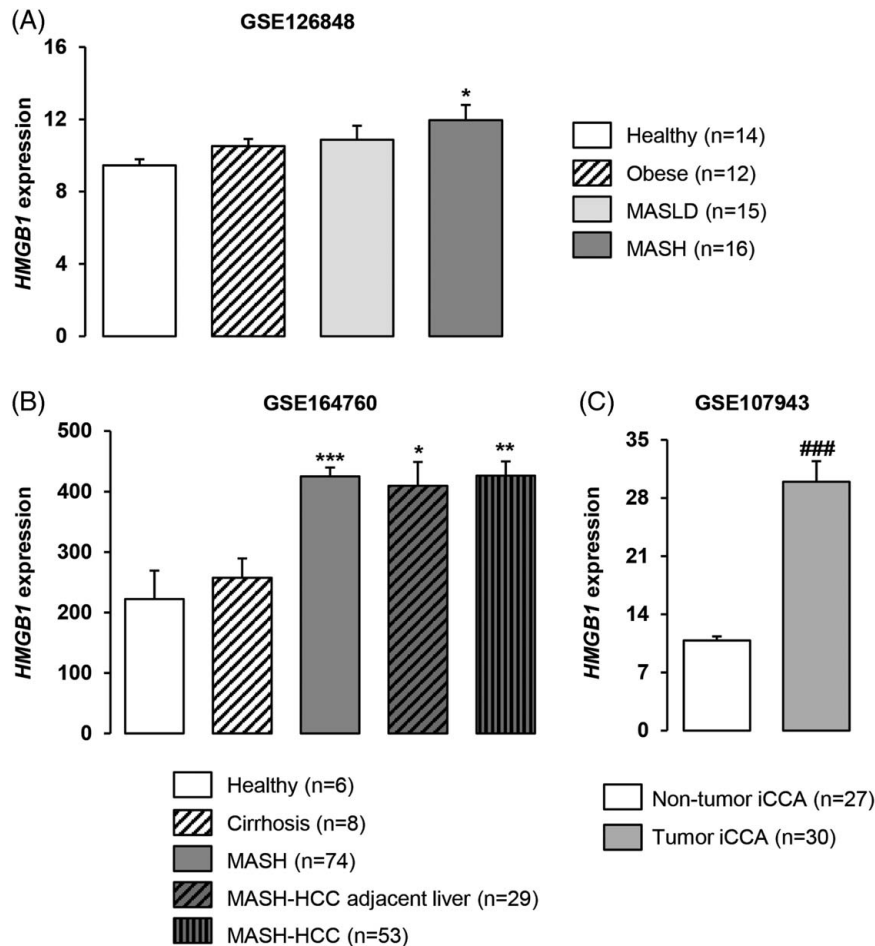
FIGURE 1 *HMGB1* expression increases in patients with MASH and liver cancer. (A–C) *HMGB1* mRNA expression in RNA-seq (GSE126848, GSE107943) and microarray (GSE164760) data sets. Raw read counts from GSE126848 were normalized to FPKM values. *HMGB1* expression was analyzed using probe "11739025_a_at" values for GSE164760 data set. Intensity values are expressed as RPKM in GSE107943. Values are given as mean $\pm$ SEM. *$p < 0.05$, **$p < 0.01$, and ***$p < 0.001$ versus healthy; ###$p < 0.05$ for tumor versus nontumor. Abbreviations: FPKM, fragments per kilobase of transcript per million mapped reads; HMGB1, high-mobility group box-1; iCCA, intrahepatic cholangiocarcinoma; MASH, metabolic dysfunction-associated steatohepatitis; MASLD, metabolic dysfunction-associated steatotic liver disease; RNA-seq, RNA-sequencing; RPKM, reads per kilobase per million mapped reads.

with no significant difference between empty and *Hmgb1* AAV8-injected male control and $Pten^{\triangle Hep}$ mice, at 9 and 3 months (Supplemental Figure S4A, B, http://links.lww.com/HC9/A649). Thus, overexpression of HMGB1 in the liver was greater at 3 months than at 9 months.

Overexpression of HMGB1 in hepatocytes increases liver tumor burden in both sexes of $Pten^{\triangle Hep}$ mice

Male and female $Pten^{\triangle Hep}$ mice, injected with empty and *Hmgb1* AAV8, developed tumors but more with *Hmgb1* AAV8 at 9 and 11 months, respectively, whereas control mice did not (Figure 3A, Supplemental Figure S5A, http://links.lww.com/HC9/A650). Liver-to-body weight ratios remained unchanged at 9 months between empty and *Hmgb1* AAV8-injected control male

mice (Figure 3B). Male and female $Pten^{\triangle Hep}$ mice injected with *Hmgb1* AAV8 had significantly increased liver-to-body weight ratios compared to empty AAV8-injected $Pten^{\triangle Hep}$ mice at 9 and 11 months, respectively, indicating increased tumor burden (Figure 3B, Supplemental Figure S5B, http://links.lww.com/HC9/A650). Serum alanine aminotransferase activity was higher in male $Pten^{\triangle Hep}$ mice at 9 months, regardless of the vector injected (Figure 3C). Overexpression of HMGB1 in male $Pten^{\triangle Hep}$ mice increased tumor number, frequency of tumors > 5 mm of diameter, and total tumor volume, compared to controls, at 9 months. In female $Pten^{\triangle Hep}$ mice injected with *Hmgb1* AAV8, besides the above, the number of tumors between 3 and 5 mm of diameter increased (Figure 3D, Supplemental Figure S5C, http://links.lww.com/HC9/A650). Overall, overexpression of HMGB1 in hepatocytes increases liver tumor burden in both sexes of $Pten^{\triangle Hep}$ mice.
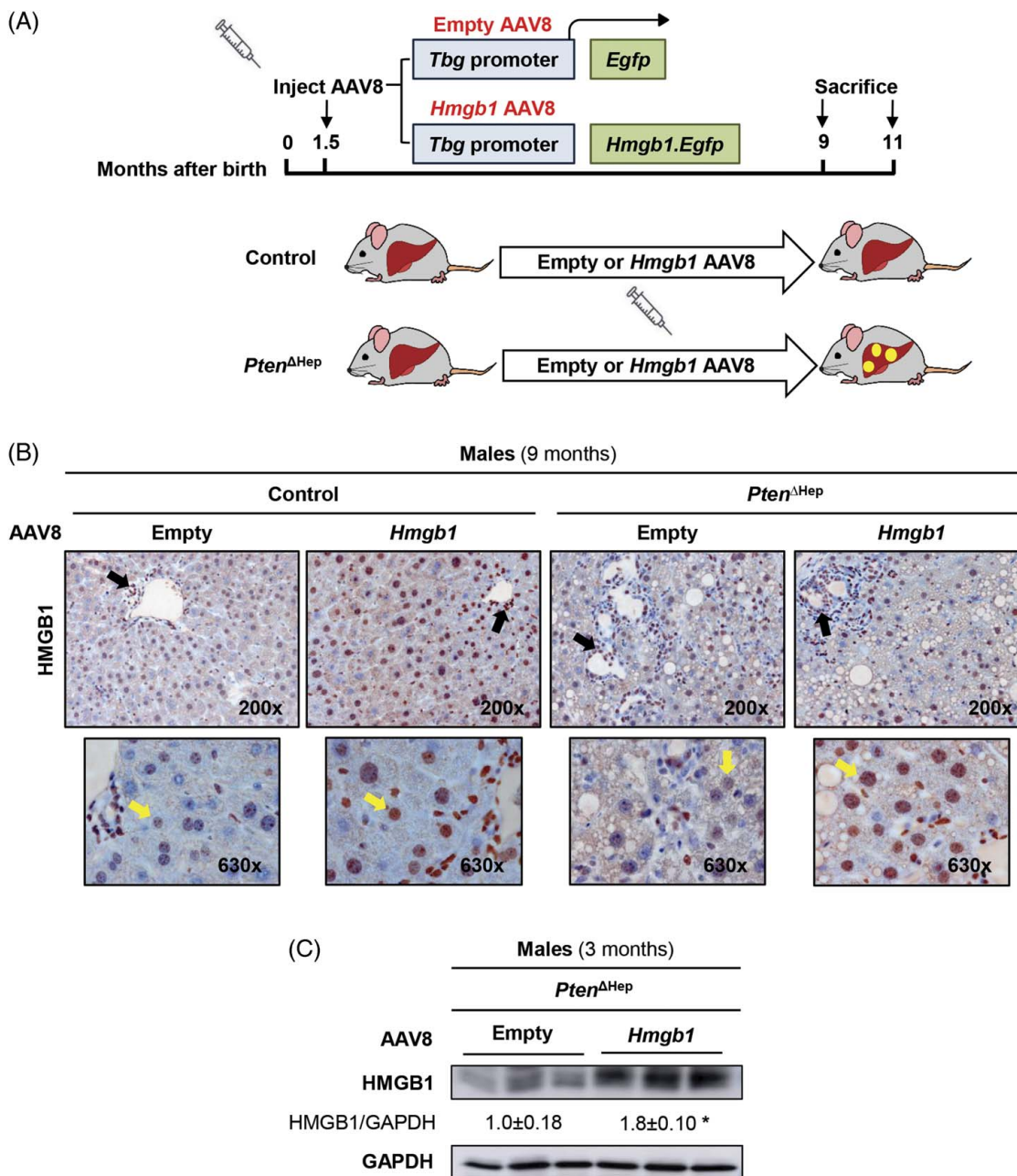
FIGURE 2 Generation of Pten$^{\Delta Hep}$ mice overexpressing HMGB1. Control and Pten$^{\Delta Hep}$ mice were generated, injected with empty or Hmgb1 AAV8 vectors through the retro-orbital vein at 1.5 months of age, and sacrificed at 9 months (males) or 11 months (females). (A) Experimental layout. (B) Liver HMGB1 immunohistochemistry (*black arrows*: HMGB1 in biliary epithelial cells; *yellow arrows*: HMGB1 in hepatocytes). (C) Western blot analysis of liver HMGB1 (n = 3/group). Values are given as mean ± SEM; *$p < 0.05$ for Hmgb1 versus empty AAV8-injected male Pten$^{\Delta Hep}$ mice. Abbreviations: AAV8, adeno-associated virus serotype-8; Egfp, enhanced green fluorescent protein; Hmgb1, high-mobility group box-1; Pten$^{\Delta Hep}$, conditional knockout mice of Pten in hepatocytes; Tbg, thyroxine-binding globulin.

Overexpression of HMGB1 in hepatocytes induces liver cancer progression in both sexes of Pten$^{\triangle Hep}$ mice

Histological analysis of liver and tumor tissues was performed to diagnose benign and malignant tumor growth. Male control mice, injected with empty or Hmgb1 AAV8, showed normal liver histology at 9 months (Supplemental Figure S6A, http://links.lww.com/HC9/A651). Approximately 83% (10/12) of male and 45% (8/11) of female Pten$^{\Delta Hep}$ mice, injected with empty AAV8, developed liver tumors, while 100% of Hmgb1 AAV8-injected male (12/12) and female (9/9) Pten$^{\Delta Hep}$ mice, developed tumors, at 9 and 11 months, respectively (Figure 4A). Histological analysis of liver tumors from empty and Hmgb1 AAV8-injected male and
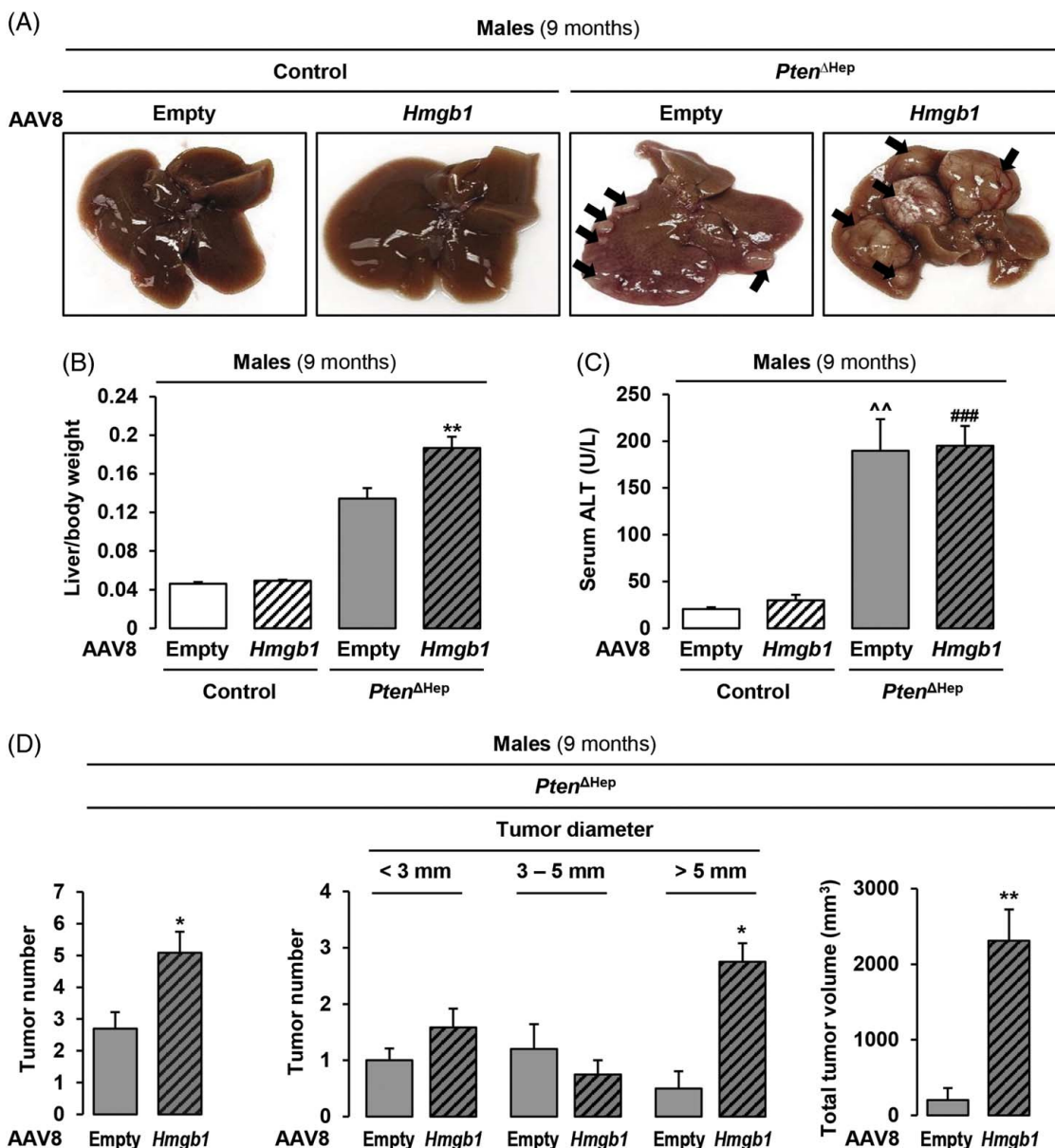
FIGURE 3 Overexpression of HMGB1 in hepatocytes increases liver tumor burden in both sexes of $Pten^{\Delta Hep}$ mice. Control and $Pten^{\Delta Hep}$ mice were generated, injected with empty or *Hmgb1* AAV8 vectors through the retro-orbital vein at 1.5 months of age, and sacrificed at 9 months (males). (A) Macroscopic appearance of the livers at 9 months (*black arrows*: tumors). (B) Liver-to-body weight ratios (control + empty AAV8 n = 6, control + *Hmgb1* AAV8 n = 5, $Pten^{\Delta Hep}$ + empty AAV8 n = 12, $Pten^{\Delta Hep}$ + *Hmgb1* AAV8 n = 12). (C) Serum ALT (n = 3/group). (D) Tumor number, tumor number according to diameter, and total tumor volume per mouse ($Pten^{\Delta Hep}$ + empty AAV8 n = 10, $Pten^{\Delta Hep}$ + *Hmgb1* AAV8 n = 12). Values are given as mean ± SEM. *$p < 0.05$ and **$p < 0.01$ for $Pten^{\Delta Hep}$ + *Hmgb1* AAV8 versus $Pten^{\Delta Hep}$ + empty AAV8; ^^$p < 0.01$ for empty AAV8-injected $Pten^{\Delta Hep}$ versus control mice; ###$p < 0.001$ for *Hmgb1* AAV8-injected $Pten^{\Delta Hep}$ versus control mice. Abbreviations: AAV8, adeno-associated virus serotype-8; *Hmgb1*, high-mobility group box-1; $Pten^{\Delta Hep}$, conditional knockout mice of *Pten* in hepatocytes.

female $Pten^{\Delta Hep}$ mice revealed the presence of HCCs, iCCAs, or mixed HCC-iCCAs (Figure 4B, Supplemental Figure S6B, http://links.lww.com/HC9/A651). Immuno-histochemical staining confirmed the presence of HCCs, iCCAs, and mixed phenotypes. iCCAs showed cytokeratin-19 staining while HCCs were positive for glypican-3. Furthermore, HCCs showed abnormal reticulin network staining[28] (Supplemental Figure 6C, http://links.lww.com/HC9/A651). In addition, $Pten^{\Delta Hep}$ mice had benign hepatic adenomas with marked steatosis and bile duct hamartomas, irrespective of treatment or sex (Supplemental Figure S6D, http://links. lww.com/HC9/A651). Nontumor and tumor tissues showed similar fibrosis regardless of injected vector (Supplemental Figure S6D, http://links.lww.com/HC9/ A651).

Only 20% (2/10) of tumor-bearing empty AAV8-injected male $Pten^{\Delta Hep}$ mice showed liver cancer
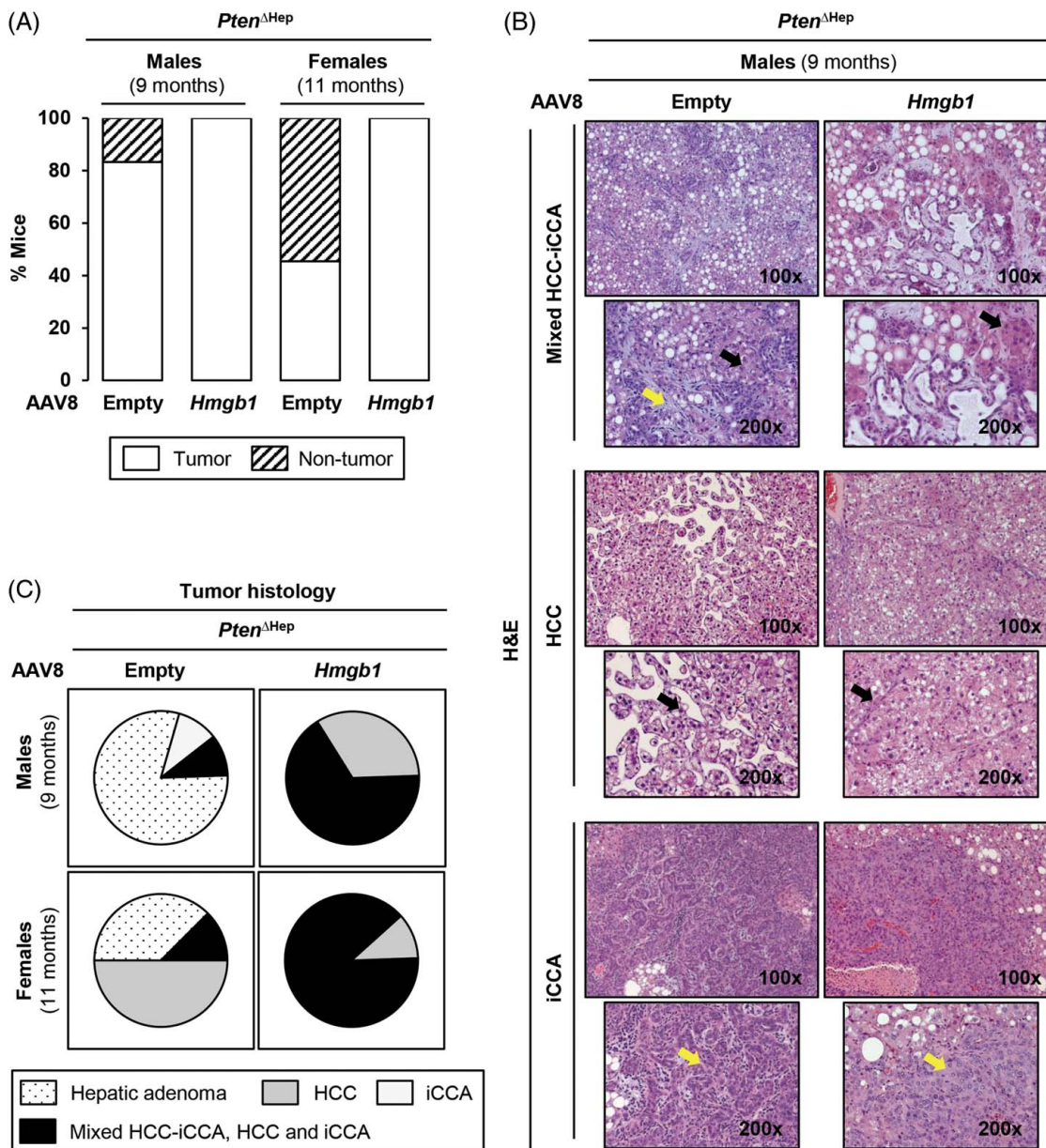
FIGURE 4 Overexpression of HMGB1 in hepatocytes induces liver cancer progression in both sexes of $Pten^{\Delta Hep}$ mice. Control and $Pten^{\Delta Hep}$ mice were generated, injected with empty or $Hmgb1$ AAV8 vectors through the retro-orbital vein at 1.5 months of age, and sacrificed at 9 months (males) or 11 months (females). (A) Tumor incidence in empty AAV8-injected $Pten^{\Delta Hep}$ (males n = 10/12, females n = 8/11) and $Hmgb1$ AAV8-injected $Pten^{\Delta Hep}$ (males n = 12/12, females n = 9/9). (B) Representative images with liver cancer histology (*black arrows*: HCCs, *yellow arrows*: iCCAs) in male $Pten^{\Delta Hep}$ mice injected with empty and $Hmgb1$ AAV8 at 9 months. (C) Pie charts indicating the percent of tumor-bearing mice with the indicated liver histology. Abbreviations: AAV8, adeno-associated virus serotype-8; $Hmgb1$, high-mobility group box-1; iCCA, intrahepatic cholangiocarcinoma; $Pten^{\Delta Hep}$, conditional knockout mice of $Pten$ in hepatocytes.

histology, with 10% developing HCC and mixed HCC-iCCA, while 10% developing only iCCA at 9 months, whereas tumors observed in the remainder mice (80%, 8/10) were benign hepatic adenomas (Figure 4C). In $Hmgb1$ AAV8-injected male $Pten^{\Delta Hep}$ mice, ~67% (8/12) had mixed HCC-iCCA along with isolated HCC and iCCA, and 33% (4/12) had only HCC (Figure 4C). In tumor-bearing empty AAV8-injected female $Pten^{\Delta Hep}$ mice, only 63% (5/8) showed liver cancer histology,

with 50% (4/8) with HCC and 13% (1/8) with mixed HCC-iCCA, at 11 months. Of the tumors observed in the remainder mice, 37% (3/8) were benign hepatic adenomas. Injection of $Hmgb1$ AAV8 resulted in 89% of mice developing mixed HCC-iCCA and isolated HCC, while 11% showed only HCC (Figure 4C). Overall, these data indicate that overexpression of HMGB1 in hepatocytes induces liver cancer progression in both sexes of $Pten^{\Delta Hep}$ mice.
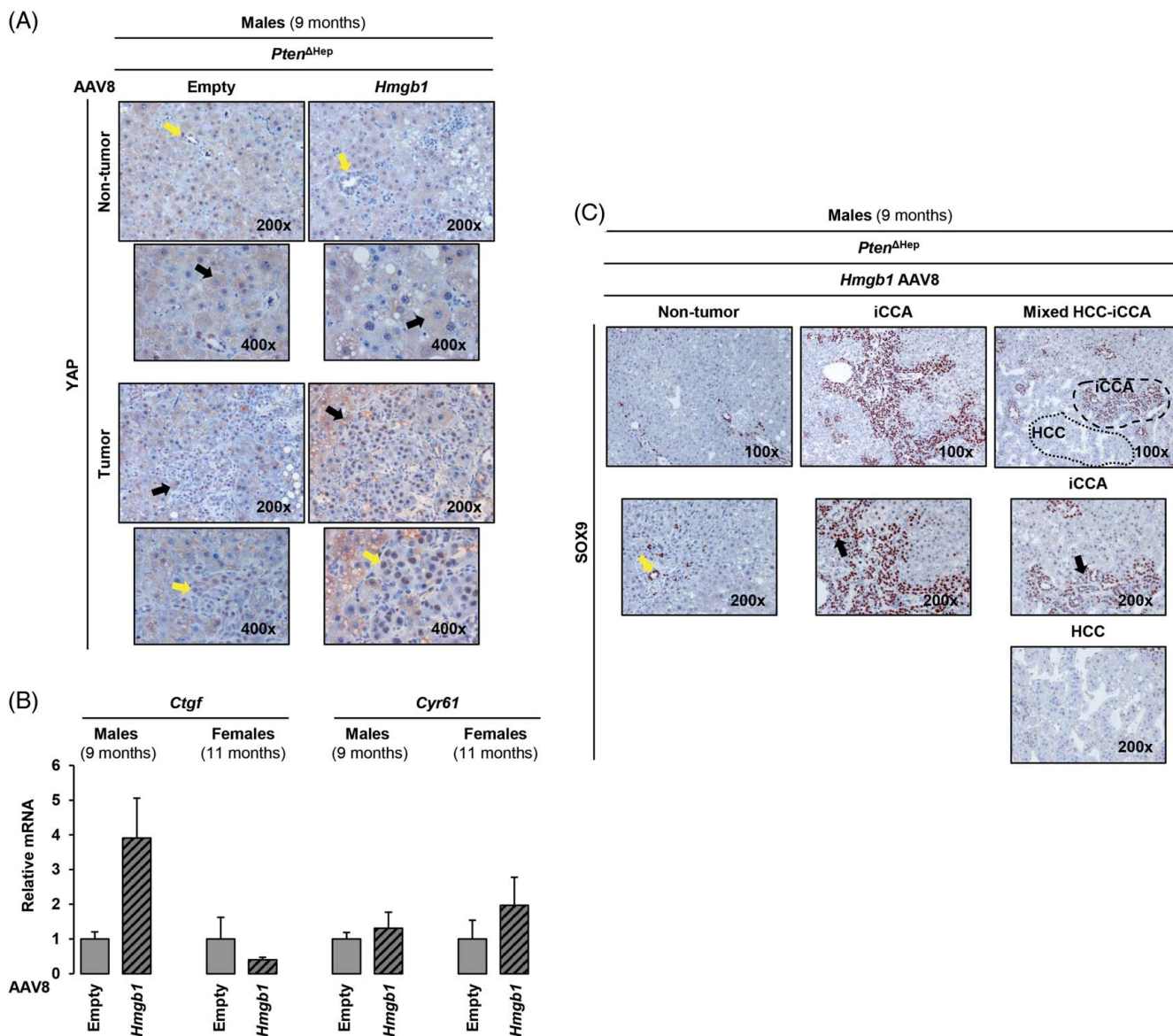
FIGURE 5 Nuclear YAP and SOX9 are present in iCCAs. Control and $Pten^{\Delta Hep}$ mice were generated, injected with empty or $Hmgb1$ AAV8 vectors through the retro-orbital vein at 1.5 months of age, and sacrificed at 9 months (males). (A) Nontumor and tumor YAP immuno-histochemistry (*black arrows*: cytoplasmic staining, *yellow arrows*: nuclear staining). (B) Relative liver mRNA levels (from tumor-adjacent tissues) of $Ctgf$ and $Cyr61$ normalized against $Gapdh$ ($Pten^{\Delta Hep}$ + empty AAV8 n = 3, $Pten^{\Delta Hep}$ + $Hmgb1$ AAV8 n = 3). (C) SOX9 immunohistochemistry in nontumor and tumor tissues (*black arrows*: SOX9+ iCCAs, *yellow arrow*: biliary epithelial cells). Values are given as mean ± SEM. Abbreviations: AAV8, adeno-associated virus serotype-8; $Ctgf$, connective tissue growth factor; $Cyr61$, cellular communication network factor-1; $Hmgb1$, high-mobility group box-1; iCCA, intrahepatic cholangiocarcinoma; $Pten^{\Delta Hep}$, conditional knockout mice of $Pten$ in hepatocytes; SOX9, sex-determining region Y-box-9; YAP; yes-associated protein.

Nuclear yes-associated protein 1A (YAP) and sex-determining region Y-box-9 (SOX9) are present in iCCAs

Most $Hmgb1$ AAV8-injected $Pten^{\Delta Hep}$ mice developed large tumors, with mixed iCCA-HCC histology (Figure 4C). A human scRNA-seq study demonstrated that the interaction of iCCA cells with the tumor microenvironment induces epigenetic changes, upregulates enhancer of zeste homolog-2, and promotes iCCA malignancy.[29] To test if overexpressing HMGB1 stimulated iCCA proliferation by enhancing enhancer of zeste homolog-2 activity, we analyzed trimethylation of lysine 27 on histone H3 (H3K27me3), a downstream target of enhancer of zeste homolog-2.[30] However, no significant change was detected, in nontumor and mixed iCCA-HCC tissues, from empty and $Hmgb1$ AAV8-injected male $Pten^{\Delta Hep}$ mice at 9 months (Supplemental Figure S7, http://links.lww.com/HC9/A652). Moreover, male $Pten^{\Delta Hep}$ mice had similar H3K27me3 expression, regardless of treatment, at 3 months (Supplemental Figure S7, http://links.lww.com/HC9/A652).

We showed that ablation of *Hmgb1* in Hippo pathway-deficient mice, reduces yes-associated protein (YAP) activity.[26] To examine if overexpression of HMGB1 supports nuclear YAP localization and activity, thus inducing liver cancer in $Pten^{\Delta Hep}$ mice, we performed YAP immunohistochemistry. In nontumor tissues from empty and *Hmgb1* AAV8-injected $Pten^{\Delta Hep}$ mice, YAP staining was cytoplasmic in hepatocytes but nuclear in biliary epithelial cells. In tumors from both treatments and in both sexes, YAP staining was nuclear in iCCAs but cytoplasmic in surrounding hepatocytes (Figure 5A and Supplemental Figure S8A, http://links.lww.com/HC9/A653). mRNA levels of YAP target genes (connective tissue growth factor (*Ctgf*), cellular communication network factor-1 (*Cyr61*)] remained unchanged in empty and *Hmgb1* AAV8-injected mice (Figure 5B). Sex-determining region Y-box-9 (SOX9) is also a direct transcriptional target of YAP.[31] Both sexes of *Hmgb1* AAV8-injected $Pten^{\Delta Hep}$ mice showed SOX9 staining only in iCCAs, while it was absent in surrounding HCCs. This suggests that YAP may be active in iCCA but not in HCC. Nontumor tissues from the same mice displayed SOX9 staining only in biliary epithelial cells (Figure 5C and Supplemental Figure S8B, http://links.lww.com/HC9/A653).

Overexpression of HMGB1 in hepatocytes increases Ki67+ and F4/80+ cells in $Pten^{\Delta Hep}$ mice

We then evaluated if accelerated liver cancer progression in *Hmgb1* AAV8-injected $Pten^{\Delta Hep}$ mice was associated with overactivation of AKT.[9] Phosphorylated AKT (S473) was barely detected in liver lysates from control mice injected with empty and *Hmgb1* AAV8. Male and female $Pten^{\Delta Hep}$ mice showed elevated AKT phosphorylation, yet no significant increase occurred between empty and *Hmgb1* AAV8-injected $Pten^{\Delta Hep}$ mice at 9 and 11 months, respectively (Figure 6A). Similarly, no difference was noted in phosphorylated protein kinase B (T308), between empty and *Hmgb1* AAV8-injected male $Pten^{\Delta Hep}$ mice (data not shown).

Next, we analyzed hepatic triglycerides to determine whether overexpression of HMGB1 induced steatosis and promoted carcinogenesis. Liver triglycerides remailed similar between *Hmgb1* and empty AAV8-injected male and female $Pten^{\Delta Hep}$ mice at 9 and 11 months, respectively (Supplemental Figure S9A, http://links.lww.com/HC9/A654). Ablation of *Pten* in the liver induces hepatic hydrogen peroxide, and thus oxidative stress.[9,32] Thiobarbituric acid-reactive substances, indicative of lipid peroxidation and oxidative stress,[33] remained unaffected in *Hmgb1* and empty AAV8-injected male and female $Pten^{\Delta Hep}$ mice at 9 and 11 months, respectively (Supplemental Figure S9B, http://links.lww.com/HC9/A654). Therefore, these results indicate that overexpression of HMGB1 in $Pten^{\Delta Hep}$ mice does not induce steatosis or oxidative stress.

Due to the role of the Wnt/β-catenin pathway in promoting liver cancer in *Pten*-null livers,[34] we evaluated the expression of components of this pathway (*Wnt3a*, *Wnt7a*, *Wnt10a*) and β-catenin protein; however, they remained similar in empty AAV8 and *Hmgb1* AAV8-injected male $Pten^{\Delta Hep}$ mice, at 9 months (Supplemental Figure S10A, B, http://links.lww.com/HC9/A655). Further, we examined hepatocyte proliferation staining nontumor and tumor liver sections for Ki67. Nontumor liver sections showed Ki67+ hyperproliferative hepatocytes in empty and *Hmgb1* AAV8-injected male $Pten^{\Delta Hep}$ mice at 3 and 9 months, but overall, the number of Ki67+ cells increased in *Hmgb1* AAV8-injected mice (Figure 6B); however, they remained unchanged in *Hmgb1* AAV8-injected female mice (Supplemental Figure S11A, http://links.lww.com/HC9/A656). Ki67+ cells were found in tumor tissues from both treated groups (Supplemental Figure S11B, http://links.lww.com/HC9/A656). Our study showed that ablation of *Hmgb1* reduced the number of F4/80+ cells in *Mst1/2*-deficient livers and was associated with reduced HCC proliferation.[26] Here, we observed increased number of F4/80+ cells, at 9 months, and increased F4/80 staining, at 3 months, in *Hmgb1* compared to empty AAV8-injected mice. Although not significant, the overall number of F4/80+ cells was increased in *Hmgb1* compared to empty AAV8-injected female $Pten^{\Delta Hep}$ mice (Figure 6C, Supplemental Figure S11C–E, http://links.lww.com/HC9/A656). Last, the expression of proinflammatory cytokines (*Ccl2, Il1β*) was tested but remained similar in both treated groups of mice (Figure 6D).

DISCUSSION

In this study, we demonstrated that overexpression of HMGB1 in hepatocytes alone does not suffice to promote liver tumorigenesis in control mice. Analysis of human microarray and RNA-seq data sets indicated increased *HMGB1* mRNA in MASH compared to healthy liver. However, a 9-month follow-up of control and $Pten^{\Delta Hep}$ mice injected with empty AAV8 showed no changes in liver and serum HMGB1, suggesting that the onset of MASH in $Pten^{\Delta Hep}$ mice is not associated with a physiological increase in HMGB1 protein expression.

We then assessed the effect of overexpressing HMGB1 in hepatocytes from $Pten^{\Delta Hep}$ mice. We observed increased overexpression of HMGB1 in hepatocytes at 3 months but not at 9 or 11 months in $Pten^{\Delta Hep}$ mice, mostly due to hepatocyte injury. $Pten^{\Delta Hep}$ mice develop MASH-like pathology with steatosis, Mallory-Denk bodies, inflammation (lymphocytes, neutrophils), and fibrosis. Moreover, $Pten^{\Delta Hep}$
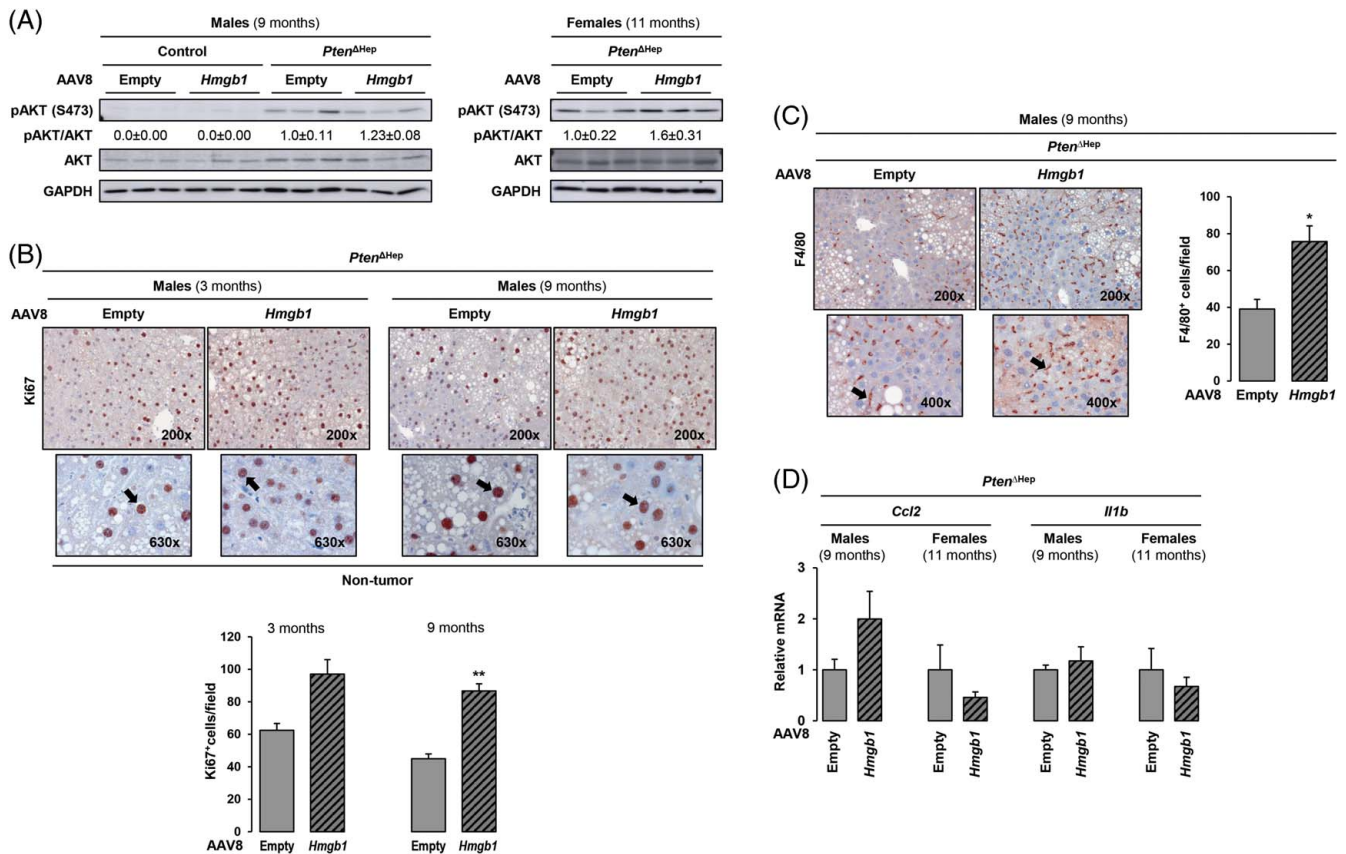
FIGURE 6 Overexpression of HMGB1 in hepatocytes increases Ki67+ and F4/80+ cells in Pten$^{\Delta Hep}$ mice. Control and Pten$^{\Delta Hep}$ mice were generated, injected with empty or Hmgb1 AAV8 vectors through the retro-orbital vein at 1.5 months of age, and sacrificed at 9 months (males) or 11 months (females). (A) Western blot analysis of pAKT (S473), AKT, and GAPDH in whole liver lysates (n = 3/group). (B) Representative images of liver Ki67 immunohistochemistry (top) (black arrows: Ki67+ nuclei). Ten 200x fields per section were used to quantify Ki67+ cells (bottom). Nontumor tissue sections are shown for Empty or Hmgb1 AAV8-treated Pten$^{\Delta Hep}$ mice. (C) Representative images of liver F4/80 immunohistochemistry (left). Ten 200x fields per section were used to quantify F4/80+ cells (right). Nontumor tissue sections are shown for Empty or Hmgb1 AAV8-treated Pten$^{\Delta Hep}$ mice. (D) Relative liver mRNA levels (from tumor-adjacent tissues) of Ccl2 and Il1β. Values are normalized against Gapdh mRNA (Pten$^{\Delta Hep}$ + empty AAV8 n = 3, Pten$^{\Delta Hep}$ + Hmgb1 AAV8 n = 3). Values are given as mean ± SEM. *$p < 0.05$ and **$p < 0.01$ for Pten$^{\Delta Hep}$ + Hmgb1 AAV8 versus Pten$^{\Delta Hep}$ + empty AAV8. Abbreviations: AAV8, adeno-associated virus serotype-8; AKT, protein kinase B; Hmgb1, high-mobility group box-1; pAKT, phosphorylated protein kinase B; Pten$^{\Delta Hep}$, conditional knockout mice of Pten in hepatocytes.

mice develop liver benign adenomas by 10–11 months of age and liver cancer by 16–18 months of age, being more prevalent in male than female Pten$^{\Delta Hep}$ mice.[9] Similarly, in our model, benign adenomas were observed irrespective of sex and treatment. Notably, 100% of Pten$^{\Delta Hep}$ mice injected with Hmgb1 AAV8 developed larger and more tumors with liver cancer histology, irrespective of sex, whereas tumors observed in mice injected control vector were benign adenomas. This underlines the role of hepatocyte-derived HMGB1 in promoting liver cancer in Pten$^{\Delta Hep}$ mice.

We proved that HMGB1 regulates YAP activity and hepatocarcinogenesis in Hippo signaling-deficient mice.[26] Deletion of Pten induces liver cancer my means of the Hippo/YAP/TAZ pathway, where deficiency of Pten and Hippo signaling accelerates metabolic dysfunction-associated steatotic liver disease and liver cancer.[35] Another study showed that Pten-deleted SOX9+ cells give rise to mixed

HCC-iCCA tumors.[36] Thus, we explored whether overexpression of HMGB1 drives liver cancer through Hippo/YAP/SOX9 activation in Pten$^{\Delta Hep}$ mice. Increased nuclear YAP staining in iCCAs in the treatment groups and the high incidence of mixed HCC-iCCAs in the Hmgb1 AAV8-injected group suggest that overexpression of HMGB1 could promote iCCA progression through YAP activation. Our data suggest minimal change in conventional YAP targets (Ctgf, Cyr61) in whole liver lysates; yet SOX9, another transcriptional target of YAP,[31] was expressed in iCCAs, suggesting that YAP activity could drive SOX9+ iCCA under overexpression of HMGB1, which needs further validation.

PTEN is a negative regulator of the PI3K/AKT pathway, and Pten-null hepatocytes show overactivation of PI3K/AKT.[7,9] Studies in a model of acute lung injury demonstrated that HMGB1 activates the PI3K/AKT pathway;[37] therefore, we hypothesized that
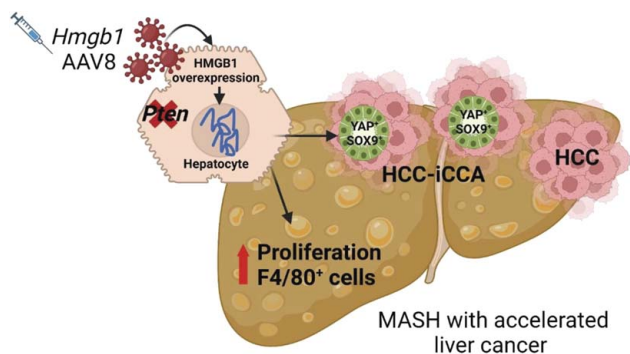
FIGURE 7 Graphical summary. Overexpression of HMGB1 in hepatocytes promotes liver cancer progression that is associated with increased cell proliferation and F4/80+ cells in *Pten*△Hep mice. The high incidence of mixed HCC-iCCA tumors and nuclear YAP and SOX9 staining in iCCAs from *Hmgb1* AAV8-treated *Pten*△Hep mice suggests that YAP activity could drive SOX9+ iCCA with overexpression of HMGB1, which needs further validation. Abbreviations: AAV8, adeno-associated virus serotype-8; *Hmgb1*, high-mobility group box-1; iCCA, intrahepatic cholangiocarcinoma; MASH, metabolic dysfunction-associated steatohepatitis.

acceleration of liver carcinogenesis in *Hmgb1* AAV8-injected *Pten*△Hep mice could be due to hyperactive AKT signaling. Injection of *Hmgb1* AAV8 did not change AKT activation, as shown by unaltered phosphorylation of S473-AKT, suggesting that overexpression of HMGB1 may act downstream of PI3K/AKT.

Pten deficiency upregulates *Wnt* signature genes and induces the Wnt/β-catenin pathway, and pharmacological blockade of this pathway reduces tumor burden by attenuating expansion of tumor-initiating cells in *Pten*△Hep mice.[34] Overexpression of HMGB1 activates Wnt/β-catenin in other cancer models.[38,39] In our study, we did not observe upregulation of *Wnt* ligands (*Wnt3a*, *Wnt7a*, *Wnt10a*) or tumor-initiating cell markers (Epcam, Sox9) (not shown), at both experimental time points or after short exposure to AAV8 vectors (3 months), indicating that overexpression of HMGB1 in hepatocytes may not drive tumor initiation and progression through activation of Wnt/β-catenin signaling. Another study demonstrated a sudden change in tumorigenic transcription factors in *Pten*△Hep compared to wild-type livers at 5 months, while their expression remained relatively stable, between 2 and 4 months.[40] Similarly, in our study, the 3- and 9-month time points chosen to analyze the mechanism underlying accelerated tumor progression may have been too early and too late, respectively. Therefore, analyzing liver tissues at additional precancer time points, between 3 and 9 months, may detect transcriptional and translational changes responsible for accelerating tumorigenesis in *Hmgb1* AAV8-injected *Pten*△Hep mice.

HMGB1 is a damage-associated molecular pattern and elicits inflammation by activating pattern-recognition receptors expressed in parenchymal and nonparenchymal cells (e.g., immune cells).[41] Binding of HMGB1 to these receptors activates the inflammasome and releases proinflammatory cytokines that mediate chronic liver disease and thus cancer development.[41,42] We showed increased F4/80+ cells in *Hmgb1* AAV8-injected *Pten*△Hep mice. These F4/80+ cells could be monocyte-derived macrophages recruited due to overexpression of HMGB1.[42] Although we did not observe significant changes in proinflammatory cytokines and chemoattractants, it is still possible that induction of other mediators of inflammation (ie, TNFα and IL17) occurs because of overexpression of HMGB1.[42] One study reported that extracellular HMGB1 activates the NFκB pathway in myeloid-derived suppressor cells, promoting their proliferation and ability to suppress antitumor activity by CD4+ and CD8+ T cells.[43] In our study, it is possible that overexpression of HMGB1 increases myeloid-derived suppressor cells, secretion of anti-inflammatory cytokines, inactivation of T cells, and promote tumorigenesis, but this needs further investigation.

In conclusion, we demonstrated that overexpression of HMGB1 in hepatocytes promotes liver cancer progression associated with increased cell proliferation and F4/80+ cells in *Pten*△Hep mice (Figure 7). However, this study remains inconclusive regarding the precise mechanism driving accelerated liver cancer growth. To explore dynamic signaling pathways involved as drivers of tumorigenesis, *Pten*△Hep livers should be evaluated at additional precancer stages such as 5 or 6 months following overexpression of HMGB1.

AUTHOR CONTRIBUTIONS

Dipti Athavale carried out the experiments and wrote the manuscript with support from Ines Barahona, Zhuolun Song, Romain Desert, Wei Chen, Hui Han, Sukanta Das, Xiaodong Ge, Sai Santosh Babu Komakula, Wei Chen, Shenglan Gao, Grace Guzman, and Natalia Nieto. Ines Barahona performed immunohistochemistry. Zhuolun Song and Daniel Lantvit helped breeding mice and performing experiments. Xiaodong Ge and Grace Guzman supervised the scoring of slides. Natalia Nieto supervised the project and obtained funding.

ACKNOWLEDGMENTS

CONFLICTS OF INTEREST

The authors have no conflicts to report.

ORCID

Dipti Athavale https://orcid.org/0000–0003–0688–4970
Ines Barahona https://orcid.org/0009–0008–8213–3339
Zhuolun Song https://orcid.org/0000–0001–5101–3950
Romain Desert https://orcid.org/0000–0001–8786–5741

Wei Chen https://orcid.org/0000–0003–3461–6658
Hui Han https://orcid.org/0000–0002–8890–4295
Sukanta Das https://orcid.org/0000–0002–2376–1174
Xiaodong Ge https://orcid.org/0000–0002–6311–8837
Sai Santosh B. Komakula https://orcid.org/0000–0001–6109–2736
Daniel Lantvit https://orcid.org/0009–0001–0963–8890
Natalia Nieto https://orcid.org/0000–0002–7941–6804

REFERENCES

1. Sia D, Villanueva A, Friedman SL, Llovet JM. Liver cancer cell of origin, molecular class, and effects on patient prognosis. Gastroenterology. 2017;152:745–61.
2. Sung H, Ferlay J, Siegel RL, Laversanne M, Soerjomataram I, Jemal A, et al. Global Cancer Statistics 2020: GLOBOCAN estimates of incidence and mortality worldwide for 36 cancers in 185 countries. CA Cancer J Clin. 2021;71:209–49.
3. Peiseler M, Tacke F. Inflammatory mechanisms underlying nonalcoholic steatohepatitis and the transition to hepatocellular carcinoma. Cancers (Basel). 2021;13:730.
4. Loomba R, Friedman SL, Shulman GI. Mechanisms and disease consequences of nonalcoholic fatty liver disease. Cell. 2021;184:2537–64.
5. European Association for the Study of the L, European Association for the Study of D, European Association for the Study of O. EASL-EASD-EASO Clinical Practice Guidelines for the management of non-alcoholic fatty liver disease. J Hepatol. 2016;64:1388–402.
6. De Lorenzo S, Tovoli F, Mazzotta A, Vasuri F, Edeline J, Malvi D, et al. Non-alcoholic steatohepatitis as a risk factor for intrahepatic cholangiocarcinoma and its prognostic role. Cancers (Basel). 2020;12:3182.
7. Morris SM, Carter KT, Baek JY, Koszarek A, Yeh MM, Knoblaugh SE, et al. TGF-beta signaling alters the pattern of liver tumorigenesis induced by Pten inactivation. Oncogene. 2015;34:3273–82.
8. Chen D, Li Z, Cheng Q, Wang Y, Qian L, Gao J, et al. Genetic alterations and expression of PTEN and its relationship with cancer stem cell markers to investigate pathogenesis and to evaluate prognosis in hepatocellular carcinoma. J Clin Pathol. 2019;72:588–96.
9. Horie Y, Suzuki A, Kataoka E, Sasaki T, Hamada K, Sasaki J, et al. Hepatocyte-specific Pten deficiency results in steatohepatitis and hepatocellular carcinomas. J Clin Invest. 2004;113:1774–83.
10. Gaskell H, Ge X, Nieto N. High-mobility group box-1 and liver disease. Hepatol Commun. 2018;2:1005–20.
11. Chandrashekaran V, Seth RK, Dattaroy D, Alhasson F, Ziolenka J, Carson J, et al. HMGB1-RAGE pathway drives peroxynitrite signaling-induced IBD-like inflammation in murine nonalcoholic fatty liver disease. Redox Biol. 2017;13:8–19.
12. Gaskell H, Ge X, Desert R, Das S, Han H, Lantvit D, et al. Ablation of Hmgb1 in intestinal epithelial cells causes intestinal lipid accumulation and reduces NASH in mice. Hepatol Commun. 2020;4:92–108.
13. Ge X, Antoine DJ, Lu Y, Arriazu E, Leung TM, Klepper AL, et al. High mobility group box-1 (HMGB1) participates in the pathogenesis of alcoholic liver disease (ALD). J Biol Chem. 2014;289:22672–91.
14. Ge X, Arriazu E, Magdaleno F, Antoine DJ, Dela Cruz R, Theise N, et al. High mobility group box-1 drives fibrosis progression signaling via the receptor for advanced glycation end products in mice. Hepatology. 2018;68:2380–404.
15. Arriazu E, Ge X, Leung TM, Magdaleno F, Lopategi A, Lu Y, et al. Signalling via the osteopontin and high mobility group box-1 axis drives the fibrogenic response to liver injury. Gut. 2017;66:1123–37.
16. Ge X, Leung TM, Arriazu E, Lu Y, Urtasun R, Christensen B, et al. Osteopontin binding to lipopolysaccharide lowers tumor necrosis factor-alpha and prevents early alcohol-induced liver injury in mice. Hepatology. 2014;59:1600–16.
17. Cubero FJ, Nieto N. Arachidonic acid stimulates TNFalpha production in Kupffer cells via a reactive oxygen species-pERK1/2-Egr1-dependent mechanism. Am J Physiol Gastrointest Liver Physiol. 2012;303:G228–39.
18. Oxidative-stress Nieto N. and IL-6 mediate the fibrogenic effects of [corrected] Kupffer cells on stellate cells. Hepatology. 2006;44:1487–501.
19. Magdaleno F, Ge X, Fey H, Lu Y, Gaskell H, Blajszczak CC, et al. Osteopontin deletion drives hematopoietic stem cell mobilization to the liver and increases hepatic iron contributing to alcoholic liver disease. Hepatol Commun. 2018;2:84–98.
20. Groszer M, Erickson R, Scripture-Adams DD, Lesche R, Trumpp A, Zack JA, et al. Negative regulation of neural stem/progenitor cell proliferation by the Pten tumor suppressor gene in vivo. Science. 2001;294:2186–9.
21. Chandler RJ, Tarasenko TN, Cusmano-Ozog K, Sun Q, Sutton VR, Venditti CP, et al. Liver-directed adeno-associated virus serotype 8 gene transfer rescues a lethal murine model of citrullinemia type 1. Gene Ther. 2013;20:1188–91.
22. Yan Z, Yan H, Ou H. Human thyroxine binding globulin (TBG) promoter directs efficient and sustaining transgene expression in liver-specific pattern. Gene. 2012;506:289–94.
23. Edge SB, Compton CC. The American Joint Committee on Cancer: The 7th edition of the AJCC cancer staging manual and the future of TNM. Ann Surg Oncol. 2010;17:1471–4.
24. Ferrell L. Malignant liver tumors that mimic benign lesions: Analysis of five distinct lesions. Semin Diagn Pathol. 1995;12:64–76.
25. Minnard EA, Fong Y. Benign and Malignant Tumors of the Liver. In: Rosenthal RA, Zenilman ME, Katlic MR, eds. Principles and Practice of Geriatric Surgery. New York, NY: Springer; 2001.
26. Athavale D, Song Z, Desert R, Han H, Das S, Ge X, et al. Ablation of high-mobility group box-1 in the liver reduces hepatocellular carcinoma but causes hyperbilirubinemia in Hippo signaling-deficient mice. Hepatol Commun. 2022;6:2155–69.
27. Stiles B, Wang Y, Stahl A, Bassilian S, Lee WP, Kim YJ, et al. Liver-specific deletion of negative regulator Pten results in fatty liver and insulin hypersensitivity [corrected]. Proc Natl Acad Sci USA. 2004;101:2082–7.
28. Yao S, Zhang J, Chen H, Sheng Y, Zhang X, Liu Z, et al. Diagnostic value of immunohistochemical staining of GP73, GPC3, DCP, CD34, CD31, and reticulin staining in hepatocellular carcinoma. J Histochem Cytochem. 2013;61:639–48.
29. Zhang M, Yang H, Wan L, Wang Z, Wang H, Ge C, et al. Single-cell transcriptomic architecture and intercellular crosstalk of human intrahepatic cholangiocarcinoma. J Hepatol. 2020;73:1118–30.
30. Zhou T, Sun Y, Li M, Ding Y, Yin R, Li Z, et al. Enhancer of zeste homolog 2-catalysed H3K27 trimethylation plays a key role in acute-on-chronic liver failure via TNF-mediated pathway. Cell Death Dis. 2018;9:590.
31. Liu Y, Zhuo S, Zhou Y, Ma L, Sun Z, Wu X, et al. Yap-Sox9 signaling determines hepatocyte plasticity and lineage-specific hepatocarcinogenesis. J Hepatol. 2022;76:652–4.
32. Zeng N, Li Y, He L, Xu X, Galicia V, Deng C, et al. Adaptive basal phosphorylation of eIF2alpha is responsible for resistance to cellular stress-induced cell death in Pten-null hepatocytes. Mol Cancer Res. 2011;9:1708–17.
33. Pan M, Cederbaum AI, Zhang YL, Ginsberg HN, Williams KJ, Fisher EA. Lipid peroxidation and oxidant stress regulate hepatic

apolipoprotein B degradation and VLDL production. J Clin Invest. 2004;113:1277–87.

34. Debebe A, Medina V, Chen CY, Mahajan IM, Jia C, Fu D, et al. Wnt/beta-catenin activation and macrophage induction during liver cancer development following steatosis. Oncogene. 2017; 36:6020–9.

35. Jeong SH, Kim HB, Kim MC, Lee JM, Lee JH, Kim JH, et al. Hippo-mediated suppression of IRS2/AKT signaling prevents hepatic steatosis and liver cancer. J Clin Invest. 2018;128:1010–25.

36. Chen J, Debebe A, Zeng N, Kopp J, He L, Sander M, et al. Transformation of SOX9 (+) cells by Pten deletion synergizes with steatotic liver injury to drive development of hepatocellular and cholangiocarcinoma. Sci Rep. 2021;11:11823.

37. Li R, Zou X, Huang H, Yu Y, Zhang H, Liu P, et al. HMGB1/PI3K/Akt/mTOR signaling participates in the pathological process of acute lung injury by regulating the maturation and function of dendritic cells. Front Immunol. 2020;11:1104.

38. Chen YC, Statt S, Wu R, Chang HT, Liao JW, Wang CN, et al. High mobility group box 1-induced epithelial mesenchymal transition in human airway epithelial cells. Sci Rep. 2016;6: 18815.

39. Wang XH, Zhang SY, Shi M, Xu XP. HMGB1 promotes the proliferation and metastasis of lung cancer by activating the Wnt/beta-catenin pathway. Technol Cancer Res Treat. 2020;19: 1533033820948054.

40. Wang G, Luo X, Liang Y, Kaneko K, Li H, Fu XD, et al. A tumorigenic index for quantitative analysis of liver cancer initiation and progression. Proc Natl Acad Sci USA. 2019;116: 26873–80.

41. Yu LX, Ling Y, Wang HY. Role of nonresolving inflammation in hepatocellular carcinoma development and progression. NPJ Precis Oncol. 2018;2:6.

42. Weston CJ, Zimmermann HW, Adams DH. The role of myeloid-derived cells in the progression of liver disease. Front Immunol. 2019;10:893.

43. Parker KH, Sinha P, Horn LA, Clements VK, Yang H, Li J, et al. HMGB1 enhances immune suppression by facilitating the differentiation and suppressive activity of myeloid-derived suppressor cells. Cancer Res. 2014;74:5723–33.